Audio Engineering Society

Convention Paper 8437

Presented at the 130th Convention
2011 May 13–16 London, UK

System Identification of Equalized Room Impulse Responses by an Acoustic Echo Canceller using Proportionate LMS Algorithms

Stefan Goetze[1], Feifei Xiong[1], Jan Ole Jungmann[2], Markus Kallinger[3], Karl-Dirk Kammeyer[4], Alfred Mertins[2]

[1] *Fraunhofer Institute for Digital Media Technology (IDMT), Project group Hearing-, Speech-, and Audio-Technology (HSA), 26129 Oldenburg, Germany*

[2] *University of Lübeck, Institute for Signal Processing, 23538 Lübeck, Germany*

[3] *Markus Kallinger contributed to this work while he was with the University of Oldenburg, 26111 Oldenburg, Germany, he is now with the Fraunhofer Institute for Integrated Circuits (IIS), 91058 Erlangen, Germany*

[4] *University of Bremen, Dept. of Communications Engineering, 28334 Bremen, Germany*

Correspondence should be addressed to Stefan Goetze (s.goetze@idmt.fraunhofer.de)

ABSTRACT

Hands-free telecommunication systems usually employ subsystems for acoustic echo cancellation (AEC), listening-room compensation (LRC) and noise reduction in combination. This contribution discusses a combined system of a two-stage AEC filter and an LRC filter to remove reverberation introduced by the listening room. An inner AEC is used to achieve initial echo reduction and to perform system identification needed for the LRC filter. An additional outer AEC is used to further reduce the acoustic echoes. The performance of proportionate filter update schemes such as the so-called proportionate normalized least mean squares algorithm (PNLMS) or the improved PNLMS (IPNLMS) for system identification of equalized impulse response (IR) are shown and the mutual influences of the subsystems are analyzed. If the LRC filter succeeds in shaping a sparse overall IR for the concatenated system of LRC filter and room impulse response (RIR), the PNLMS performs best since it is optimized for the identification of sparse IRs. However, the equalization may be imperfect due to channel estimation errors in periods of convergence and due to the so-called tail-effect of AEC, i.e. the fact that only the first part of an RIR is identified in practical systems. The IPNLMS is more appropriate in this case to identify the equalized IR.

1. INTRODUCTION

Hands-free systems usually use strategies to cope with disturbances like ambient noise, acoustic echoes and reverberation [1]. A block diagram of such a hands-free system which will be discussed in this contribution is shown in Fig. 1. It contains a listening-room compensation (LRC) filter $\mathbf{c}_{\mathrm{EQ}}[k]$ to reduce reverberation caused by the room impulse response (RIR) $\mathbf{h}[k]$ and an acoustic echo cancellation filter $\mathbf{c}_{\mathrm{AEC}}[k]$ that can be used for identification of the RIR as well as identification of the concatenated system of LRC filter $\mathbf{c}_{\mathrm{EQ}}[k]$ and RIR $\mathbf{h}[k]$.

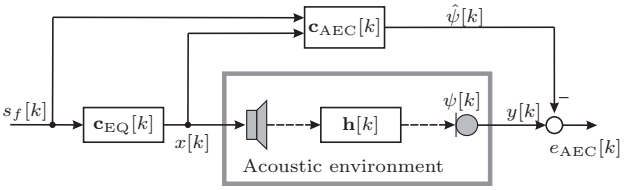

Fig. 1: Block diagram of a hands-free system containing LRC filter $\mathbf{c}_{\mathrm{EQ}}[k]$ and AEC filter $\mathbf{c}_{\mathrm{AEC}}[k]$. The AEC filter can be used to identify the RIR $\mathbf{h}[k]$ (*inner AEC*) and/or the IR of the concatenated system of RIR and equalizer (*outer AEC*).

Acoustic echoes arise from the acoustic coupling between loudspeaker and microphone in a hands-free scenario that can be described mathematically by the RIR $\mathbf{h}[k]$. The speech signal of the far-end user $s_f[k]$ is pre-filtered by the equalizer, played back by the near-end loudspeaker and picked up again by the near-end microphone. Thus, a filtered version of the far-end signal $s_f[k]$ would be transmitted back to the far-end listener. By this, the far-end user hears his or her own voice delayed by the round-trip delay of the system if no counter-measures are taken, which heavily disturbs natural speech communication [1]. Acoustic echo cancellers are able to estimate and subtract the echo part $\psi[k]$ from the microphone signal $y[k]$. Note that, in general, the acoustic echo $\psi[k]$ is superimposed by the near-end speaker $s_n[k]$, i.e. the signal which is to be transmitted to the far-end side, and an ambient noise signal $n[k]$. Both are neglected in Fig. 1 as well as in the remainder of this paper for simplicity reasons. Influences of noise and near-end speaker are beyond the scope of this paper and extensively discussed in the literature, cf. e.g. [1, 2]. If single-channel systems are used, echo cancellation is achieved by system identification, i.e. estimation of the acoustic channel $\mathbf{h}[k]$ by the AEC $\mathbf{c}_{\mathrm{AEC}}[k]$.

A further disturbance in hands-free systems is reverberation, introduced to the speech signal due to numerous reflections at the room boundaries. Reverberant signals sound distant and echoic, like it is known from listening to speech e.g. in churches or large halls [3, 4]. LRC filters can be applied to remove the reverberant part of the signal at the position of the near-end listener by pre-filtering the loudspeaker signal [5, 6, 7] as shown in Fig. 1. This dereverberation approach is known as listening-room compensation (LRC). Knowledge about the acoustic channel is often assumed for designing the LRC filter which is not available in real-world systems [8, 9]. An estimate of the acoustic channel can be obtained by an *inner AEC* in parallel to the RIR. Furthermore, an *outer AEC* can further reduce the acoustic echo $\psi[k]$. To achieve this, the *outer AEC* has to identify the equalized acoustic channel, which is mathematically defined by the convolution of LRC filter $\mathbf{c}_{\mathrm{EQ}}[k]$ and RIR $\mathbf{h}[k]$. The *outer AEC* may observe a sparse IR if the LRC filter performs well, i.e. a delayed delta function could be achieved for the case of perfect equalization. In this case so-called proportionate update schemes [10, 11, 12, 13] known from the field of network echo cancellation [14] can be applied for the *outer AEC* since they are able to converge faster at coefficients that observe high energy at the specific lag of the IR.

Notation: The following notation is used throughout the paper. Vectors and matrices are printed in boldface while scalars are printed in italic. The superscripts $(\cdot)^T$ and $(\cdot)^+$ denote the transposition and the Moore-Penrose pseudoinverse, respectively. The operator $*$ denotes the convolution of two sequences, $\mathrm{E}\{\cdot\}$ is the expectation operator, and the operator $\mathrm{convmtx}\{\mathbf{h}, L_{\mathrm{EQ}}\}$ generates a convolution matrix of size $(L_{\mathrm{EQ}} + L_h - 1) \times L_{\mathrm{EQ}}$. The operator $\mathrm{diag}\{\cdot\}$ yields a matrix of size $L \times L$ from a vector of size $L \times 1$ that has the vector's elements on its main diagonal and zeros elsewhere.

The remainder of this paper is organized as follows: Section 2 briefly describes the concept of LRC and Section 3 introduces the algorithms used for system identification in this contribution. Possibilities for combination of the two sub-systems are discussed in

Section 4. Simulation results compare the discussed approaches in Section 5, and Section 6 concludes the paper.

2. LISTENING-ROOM COMPENSATION

Although equalization of RIRs has been research topic for quite some time now [15] it is still an active research field due to the non-trivial inherent difficulties: RIRs are non-minimum phase systems, in general, which leads to the fact that no exact stable and causal systems exists for inversion [15]. The length of common RIRs makes their equalization computationally demanding even if FIR approximation approaches are used. Furthermore, room transfer functions (RTFs) are characterized by various notches in the frequency-domain, caused by numerous zeros very close to or even outside the unit circle in z-domain [16]. This leads to insufficient robustness of most LRC approaches in terms of spatial robustness and robustness to RIR identification errors [17]. Even if mathematically satisfying results are obtained by LRC filters small residual distortions in the equalized IR may be clearly perceivable and highly disturbing [**?**, 18].

To tackle the problem of computational effort and to be able to track changes of time-varying RIR, gradient algorithms for equalization have been proposed [19, 20, 21]. In this paper we use the decoupled filtered-X least-mean-squares (dFxLMS) algorithm from [20] which is an extension of the modified filtered-X least-mean-squares (mFxLMS) [22] and allows for an increased convergence speed (cf. [20] for details).

In a common LRC setup, the LRC filter precedes the acoustic channel, as shown in Fig. 1.

To obtain the filter coefficients of the equalizer of order L_{EQ}

$$\mathbf{c}_{\mathrm{EQ}}[k] = \left[c_{\mathrm{EQ},0}[k], c_{\mathrm{EQ},1}[k], ..., c_{\mathrm{EQ},L_{\mathrm{EQ}}-1}[k]\right]^T, \quad (1)$$

generally the squared system distance between the concatenated system of equalizer $\mathbf{c}_{\mathrm{EQ}}[k]$ and the RIR

$$\mathbf{h}[k] = [h_0[k], h_1[k], ..., h_{L_h-1}[k]]^T \quad (2)$$

is minimized:

$$\underset{\mathbf{c}_{\mathrm{EQ}}}{\operatorname{argmin}} ||\mathbf{H}[k]\mathbf{c}_{\mathrm{EQ}}[k] - \mathbf{d}||^2 \ . \quad (3)$$

In (3)

$$\mathbf{H}[k] = \mathrm{convmtx}\left\{\mathbf{h}[k], L_{\mathrm{EQ}}\right\} \quad (4)$$

is the convolution matrix obtained by the coefficients of the RIR, and

$$\mathbf{d} = [\underbrace{0, ..., 0}_{k_0}, d_0, d_1, ..., d_{L_d-1}, \underbrace{0, ..., 0}_{L_h+L_{\mathrm{EQ}}-1-L_d-k_0}]^T \quad (5)$$

is the desired system vector which is usually chosen as a delayed delta function, a delayed band-pass or a delayed high-pass [23]. A straightforward solution of (3) leads to the well-known least-squares equalizer [**?**]

$$\mathbf{c}_{\mathrm{EQ}} = \mathbf{H}^{+}\mathbf{d}. \quad (6)$$

Due to the generally high LRC filter length L_{EQ} the calculation of the Moore-Penrose pseudoinverse in (6) leads to a high computational effort, which can be significantly reduced by the gradient approach descibed in [20] and depicted in Fig. 2.

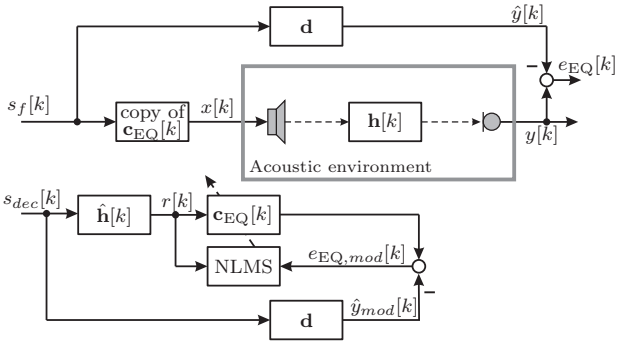

Fig. 2: Block diagram of LRC system with decoupled filtered-X least-mean-squares (dFxLMS) algorithm.

By using a modified error signal $e_{\mathrm{EQ},mod}[k]$ compared to the conventional filtered-X least-mean-squares (FxLMS) that uses the error signal $e_{\mathrm{EQ}}[k]$ the update branch of the algorithm can be designed without any coupling to the system output $y[k]$. Please note that the update path is nevertheless influenced by the system $\mathbf{h}[k]$ that is to be equalized, for the dFxLMS update scheme shown in Fig. 2 in terms of the RIR estimate

$$\hat{\mathbf{h}}[k] = \left[\hat{h}_0[k], \hat{h}_1[k], ..., \hat{h}_{L_h-1}[k]\right]^T. \quad (7)$$

See Sections 3 and 4 for RIR estimation by means of the acoustic echo canceller (AEC) filters described there.

Instead of depending on the signal statistics of the input signal $s_f[k]$ the update path is driven by an excitation signal $s_{dec}[k]$ which can be optimized to achieve higher convergence speed for the filter $\mathbf{c}_{\mathrm{EQ}}[k]$. Furthermore, an overclocking factor O is introduced that allows for further increase of the convergence speed at cost of higher computational effort by calculating O filter updates for each input sample of $s_f[k]$. In this contribution a white Gaussian excitation is chosen for $s_{dec}[k]$. See [20] for more details. The dFxLMS can be summarized as follows.

Algorithm 1 Decoupled filtered-X LMS algorithm.

1: **for** $i = 0 : O-1$ **do**
2: $\quad \mathbf{r}[k+i] = \hat{\mathbf{H}}^T[k]\mathbf{s}_{dec,L_{\hat{h}}}[k+i]$
3: $\quad e_{\mathrm{EQ},mod}[k+i] = \mathbf{r}^T[k+i]\mathbf{c}_{\mathrm{EQ}}[k+i] - \mathbf{s}^T_{dec,L_h}[k+i]\mathbf{d}$
4: $\quad \mathbf{c}_{\mathrm{EQ}}[k+i+1] = \mathbf{c}_{\mathrm{EQ}}[k+i] + \mu' \mathbf{r}[k+i] e_{\mathrm{EQ},mod}[k+i]$
5: **end for**
6: Copy updated EQ coefficients $\mathbf{c}_{\mathrm{EQ}}[k+i+1]$ to upper branch

$\hat{\mathbf{H}}[k] = \mathrm{convmtx}\left\{\hat{\mathbf{h}}[k], L_{\mathrm{EQ}}\right\}$ denotes the convolution matrix obtained by the RIR estimate $\hat{\mathbf{h}}[k]$ in Algorithm 1 . The input signal vectors $\mathbf{s}_{dec,L_{\hat{h}}}[k]$ and $\mathbf{s}_{dec,L_h}[k]$ only differ in length to match the vector and matrix products in Algorithm 1 and are defined as follows:

$$\mathbf{s}_{dec,L_{\hat{h}}}[k] = \left[s_{dec}[k], ..., s_{dec}[k - L_{\hat{h}} - L_{\mathrm{EQ}} + 2]\right]^T, \quad (8)$$

$$\mathbf{s}_{dec,L_h}[k] = \left[s_{dec}[k], ..., s_{dec}[k - L_h - L_{\mathrm{EQ}} + 2]\right]^T. \quad (9)$$

3. ACOUSTIC ECHO CANCELLERS FOR LRC SYSTEM IDENTIFICATION

Since in real-world systems knowledge of the RIR is not available it has to be identified by adaptive algorithms. Furthermore, adaptive tracking of the RIR estimate is necessary since the RIR is time-varying in general. The system identification to obtain $\hat{\mathbf{h}}[k]$ in (7) can be done by an acoustic echo cancellation filter [9] as shown in Fig. 3. Estimation errors are, however, inevitable, e.g. in periods of initial convergence or after RIR changes.

As illustrated in Fig. 3 the RIR $\mathbf{h}[k]$ can be split up into one part $\hat{\mathbf{h}}[k]$ which is correctly identified by the AEC and an estimation error $\tilde{\mathbf{h}}[k]$:

$$\mathbf{h}[k] = \begin{bmatrix} \hat{\mathbf{h}}[k] \\ \mathbf{0} \end{bmatrix} + \tilde{\mathbf{h}}[k] = \begin{bmatrix} \mathbf{c}_{\mathrm{AEC}}[k] \\ \mathbf{0} \end{bmatrix} + \tilde{\mathbf{h}}[k] \quad (10)$$

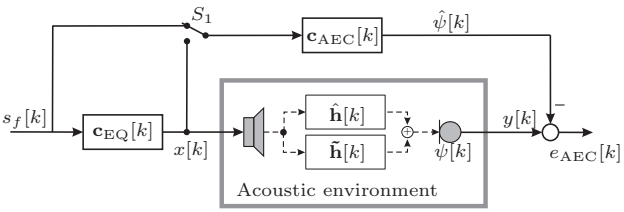

Fig. 3: Block diagram of LRC filter $\mathbf{c}_{\mathrm{EQ}}[k]$ and AEC filter $\mathbf{c}_{\mathrm{AEC}}[k]$. The RIR $\mathbf{h}[k]$ can be split up into a part $\hat{\mathbf{h}}[k]$ which is correctly modeled by the AEC and the AEC system misalignment $\tilde{\mathbf{h}}[k]$ (estimation error). S_1 switches between *inner AEC* for identification of $\mathbf{h}[k]$ and *outer AEC* for identification of the concatenated system of RIR and equalizer.

$$\mathbf{c}_{\mathrm{AEC}}[k] = \left[c_{\mathrm{AEC},0}[k],\ ...,\ c_{\mathrm{AEC},L_{\mathrm{AEC}}-1}[k]\right]^T \quad (11)$$

$$\hat{\mathbf{h}}[k] = \mathbf{c}_{\mathrm{AEC}}[k] \quad (12)$$

$$\tilde{\mathbf{h}}[k] = \left[\tilde{h}_0[k]\,,\ ...\,,\ \tilde{h}_{L_h-1}[k]\right]^T \quad (13)$$

Since L_{AEC} is in general smaller than the length of the RIR L_h the so-called tail of the RIR cannot be identified by the AEC and, thus, always contributes to the estimation error $\tilde{\mathbf{h}}[k]$. This problem is commonly known as *tail-effect* of AEC [24, 25].

3.1. Proportionate Normalized LMS Algorithm

Besides conventional AEC updates schemes like e.g. the normalized least-mean-squares (NLMS) algorithms so-called proportionate update schemes exist which have been originally developed for network acoustic echo cancellation and lead to faster convergence if the IR which has to be identified is sparse, i.e. if a large percentage of the energy of the IR is concentrated at a small percentage of coefficients. For the case of a perfectly equalized RIR the concatenated system of RIR and equalizer would equal to the desired system $\mathbf{d}$ which is sparse if chosen to be a delayed delta function, band-pass or high-pass. Fig. 4 shows four IRs that will be analyzed in this paper exemplarily. The delayed unit impulse $h_1(t)$ depicted in Fig. 4 (a) obviously is characterized by the highest sparsity, yielding a sparsity measure [13]

$$\xi(\mathbf{h}) = \frac{L_h}{L_h - \sqrt{L_h}} \left(1 - \frac{\|\mathbf{h}\|_1}{\sqrt{L_h}\|\mathbf{h}\|_2}\right) \quad (14)$$

of $\xi = 1$. In (14) $\|\mathbf{h}\|_1$ and $\|\mathbf{h}\|_2$ are the ℓ_1- and ℓ_2-norms of $\mathbf{h}$, respectively. Two common RIRs $h_2(t)$

and $h_3(t)$ having different reverberation times $\tau_{60} = \{100, 500\}$ ms are depicted in Fig. 4 (b) and (c). The IR depicted in Fig. 4 (d) is the result of an equalization of $h_3(t)$ by the least-squares equalizer in (6) with $L_{\mathrm{EQ}} = 2048$ at a sampling rate of $f_s = 8000$ Hz. It can be seen from Fig. 4 (d) that sparse IRs can be achieved by equalization and, thus, the application of proportionate filter update schemed may be advantageous.

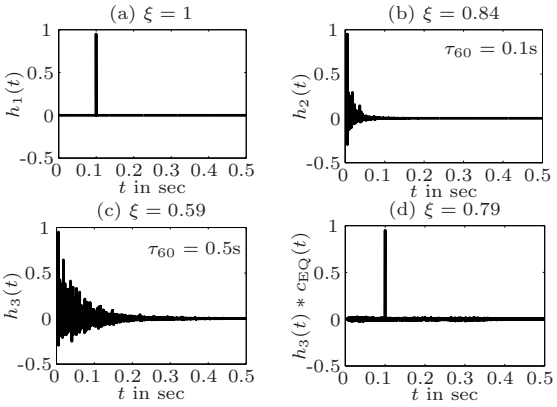

Fig. 4: Examples of IRs that have to be identified by an AEC.

The proportionate normalized least-mean-squares (PNLMS) algorithm [10, 26] differs from the NLMS algorithm by the fact that the available adaptation energy is distributed unevenly over all filter coefficients, i.e. each coefficient is updated with an adaptation gain proportional to its own magnitude. The underlying idea was originally presented in [27] based on the assumption that typical RIRs decay exponentially. Since in practice, the real magnitude of each coefficient is not known in advance for arbitrary IRs, the current LRC filter coefficients will be used in the PNLMS approach instead.

The proportionate idea is realized by introducing a coefficient-dependent step size matrix $\mathbf{M}_{\mathrm{P}}[k]$. The algorithm is summarized in the following according to the definitions in [26] which are slightly modified compared to the original proposal of the PNLMS of [10]. Please refer to [26] for a more elaborate discussion of proportionate coefficient updates as well as for the choice of the algorithm's parameters υ and ρ. For our simulations we chose $\upsilon = 0.01$, $\rho = 5/L_{\mathrm{AEC}}$, $\delta_{\mathrm{P}} = \delta_{\mathrm{NLMS}}/L_{\mathrm{AEC}}$ and $\delta_{\mathrm{NLMS}} = 0.01$.

Algorithm 2 Proportionate normalized LMS (PNLMS) algorithm.

$\hat{\psi}[k] = \sum_{i=0}^{L_{\mathrm{AEC}}-1} c_{\mathrm{AEC},i}[k]\, x[k-i]$
$e_{\mathrm{AEC}}[k] = \psi[k] - \hat{\psi}[k]$
$l_\infty[k] = \max\{|c_{\mathrm{AEC},0}[k]|, \ldots, |c_{\mathrm{AEC},L_{\mathrm{AEC}}-1}[k]|\}$,
$l'_\infty[k] = \max\{\upsilon, l_\infty[k]\}$
for $i = 0$ to $L_{\mathrm{AEC}} - 1$ **do**
  $\mu'_{\mathrm{P},i}[k] = \max\{\rho\, l'_\infty[k], |c_{\mathrm{AEC},i}[k]|\}$
end for
$\bar{\mu}'_{\mathrm{P}}[k] = \frac{1}{L_{\mathrm{AEC}}} \sum_{i=0}^{L_{\mathrm{AEC}}-1} \mu'_{\mathrm{P},i}[k]$
$\mathbf{M}_{\mathrm{P}}[k] = \mathrm{diag}\left\{\left[\frac{\mu'_{\mathrm{P},0}[k]}{\bar{\mu}'_{\mathrm{P}}[k]}, \ldots, \frac{\mu'_{\mathrm{P},L_{\mathrm{AEC}}-1}[k]}{\bar{\mu}'_{\mathrm{P}}[k]}\right]\right\}$
$\mathbf{c}_{\mathrm{AEC}}[k+1] = \mathbf{c}_{\mathrm{AEC}}[k] + \mu[k] \frac{\mathbf{M}_{\mathrm{P}}[k]\,\mathbf{x}[k]\, e_{\mathrm{AEC}}[k]}{\mathbf{x}^T[k]\mathbf{M}_{\mathrm{P}}[k]\mathbf{x}[k] + \delta_{\mathrm{P}}}$

In comparison to the NLMS algorithm, the PNLMS algorithm's initial convergence and tracking is very fast if the IR which is to be identified is sparse. Unfortunately, for dispersive IRs, the PNLMS converges even slower than the NLMS algorithm [26].

3.2. Improved Proportionate Normalized LMS Algorithm

To avoid the above mentioned deficiency of the PNLMS algorithm, generalized update schemes were proposed that combined the idea of proportionate filter updates with conventional NLMS updates [11, **?**, 28]. One of these algorithms that shall be introduced briefly is the so-called improved proportionate NLMS (IPNLMS) algorithm [28].

The IPNLMS algorithm is summarized as follows:

Algorithm 3 Improved proportionate normalized LMS (IPLMS) algorithm.

$\hat{\psi}[k] = \sum_{i=0}^{L_{\mathrm{AEC}}-1} c_{\mathrm{AEC},i}[k]\, x[k-i]$
$e_{\mathrm{AEC}}[k] = \psi[k] - \hat{\psi}[k]$
for $i = 0$ to $L_{\mathrm{AEC}} - 1$ **do**
  $\mu_{\mathrm{IP},i}[k] = \frac{1-\alpha}{2L_{\mathrm{AEC}}} + (1+\alpha)\frac{|c_{\mathrm{AEC},i}[k]|}{2\|\mathbf{c}_{\mathrm{AEC}}[k]\|_1 + \varepsilon}$
end for
$\mathbf{M}_{\mathrm{IP}}[k] = \mathrm{diag}\left\{\left[\mu_{\mathrm{IP},0}[k], \ldots, \mu_{\mathrm{IP},L_{\mathrm{AEC}}-1}[k]\right]\right\}$
$\mathbf{c}_{\mathrm{AEC}}[k+1] = \mathbf{c}_{\mathrm{AEC}}[k] + \mu[k] \frac{\mathbf{M}_{\mathrm{IP}}[k]\,\mathbf{x}[k]\, e_{\mathrm{AEC}}[k]}{\mathbf{x}^T[k]\mathbf{M}_{\mathrm{IP}}[k]\mathbf{x}[k] + \delta_{\mathrm{IP}}}$

It differs from NLMS algorithm and PNLMS algorithm by the fact that the coefficient-dependent step-size matrix $\mathbf{M}_{\mathrm{IP}}[k]$ can be adapted to evenly spread the coefficient update speed over all coefficients as the NLMS algorithm does or to tend towards the proportionate update of the PNLMS al-

gorithm by adjusting $-1 \leq \alpha < 1$ in Line 4 in Algorithm 3. For $\alpha = -1$ it can easily be checked that the IPNLMS algorithm is identical to the NLMS algorithm and for α close to 1 the IPNLMS acts similar to the PNLMS. ε is a small positive number, chosen as $\varepsilon = 10^{-5}$ and $\delta_{\mathrm{IP}} = \delta_{\mathrm{NLMS}}/(2L_{\mathrm{AEC}})$ [28].

4. SYSTEM COMBINATION

Since as well AEC as LRC have to be updated adaptively to track RIR changes they mutually influence each other. Such influences will be discussed in this section by analyzing two possible ways to combine AEC and LRC filters. Fig. 5 shows the combined system consisting of two AEC filters $\mathbf{c}_{\mathrm{AEC}_1}[k]$ and $\mathbf{c}_{\mathrm{AEC}_2}[k]$ and the LRC filter $\mathbf{c}_{\mathrm{EQ}}[k]$.

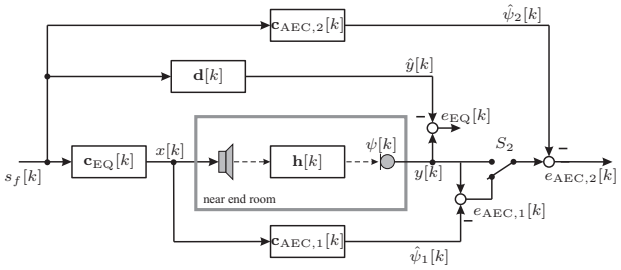

Fig. 5: Block diagram of the combined system.

We use the dFxLMS algorithm to adapt the LRC filter as described in Section 2. Please note that for simplicity reasons the update path of the dFxLMS algorithm is not shown in Fig. 5. The *inner AEC* $\mathbf{c}_{\mathrm{AEC},1}[k]$ provides an RIR estimate $\hat{\mathbf{h}}[k]$ of length L_{AEC} using an NLMS algorithm by minimizing the mean squared error signal $\mathrm{E}\{|e_{\mathrm{AEC},1}[k]|^2\}$. This estimate is needed for the LRC filter calculation in any case (cf. Fig. 2 in Section 2).

An additional *outer AEC* $\mathbf{c}_{\mathrm{AEC},2}[k]$ can be used to achieve further echo reduction. The *outer AEC* $\mathbf{c}_{\mathrm{AEC},2}[k]$ can either exploit the error signal of the *inner AEC* $e_{\mathrm{AEC},1}[k] = \psi[k] - \hat{\psi}_1[k]$ or work directly on the microphone signal $y[k]$. This can be chosen by switch S_2 in Fig. 5. It could be assumed that the echo reduction task for the *outer AEC* would be *easier* if the *inner AEC* already achieved a certain echo reduction. However, the *outer AEC* has to track changes caused by adaptation of *inner AEC* and LRC filter. Therefore a sufficiently fast adaptation is needed for the *outer AEC* especially since also the inner filters need to adapt as fast as possible, e.g. since an RIR estimate is needed quickly for the LRC filter. To achieve a higher amount of echo reduction than the *inner AEC* alone the filter length of the *outer AEC* should be greater of that of the *inner AEC* which unfortunately leads to a decreased convergence speed [24]. Here, proportionate update schemes can be a solution.

Please note that depending on S_2 in Fig. 5 the system to be identified by the *outer AEC* is either the equalized system

$$\mathbf{g}[k] = \mathbf{C}_{\mathrm{EQ}}[k]\mathbf{h}[k] \tag{15}$$

or the concatenated system of LRC filter and system distance of the *inner AEC*

$$\mathbf{g}'[k] = \mathbf{C}_{\mathrm{EQ}}[k]\left(\mathbf{h}[k] - \left[\mathbf{c}_{\mathrm{AEC},1}^T[k], \mathbf{0}^T\right]^T\right) \tag{16}$$

$$= \mathbf{C}_{\mathrm{EQ}}[k]\tilde{\mathbf{h}}_1[k] \tag{17}$$

with $\mathbf{C}_{\mathrm{EQ}}[k] = \mathrm{convmtx}\{\mathbf{c}_{\mathrm{EQ}}[k], L_h\}$. For the latter case the equalized system may not be sparse as it will be shown in Section 5.

5. SIMULATION RESULTS

Simulation results for the previously discussed problems will be shown in the following. In Section 5.1 the performance of proportionate filter update will be analyzed in general for different types of IRs. Afterwards, the mutual influences of the subsystems will be evaluated, firstly the performance of the LRC filter in dependence of the convergence of the *inner AEC* in Section 5.2 and secondly the influence of the LRC filter on the *inner AEC* in Section 5.3. The question how to combine the *outer AEC* to the overall system and the overall performance of the combined system consisting of LRC filter and both AECs will be discussed in Section 5.4.

5.1. Performance of Proportionate Update Schemes

Figs. 6 to 9 compare the performance for NLMS, PNLMS and IPNLMS update for the IRs depicted in Fig. 4 in terms of the relative system distance

$$D_{\mathrm{dB}}[k] = 10 \cdot \log_{10} \frac{||\tilde{\mathbf{h}}[k]||_2^2}{||\mathbf{h}[k]||_2^2} \tag{18}$$

and the echo return loss enhancement (ERLE) measure

$$\mathrm{ERLE} = 10\ \log_{10} \frac{\mathrm{E}\{\psi^2[k]\}}{\mathrm{E}\{e^2_{\mathrm{AEC}}[k]\}}. \qquad (19)$$

The first 1500 coefficients of the corresponding IR are depicted in panel (a) of Figs. 6 to 9. The RIR length was $L_h = 4096$ and the AEC filter length $L_{\mathrm{AEC}} = 1024$ at a sampling rate of $f_s = 8000$ Hz. For the IPNLMS, α was chosen to $\alpha = 0$ and $\delta_{\mathrm{NLMS}} = 0.01$ for all algorithms. ERLE and relative system distances are shown for a white Gaussian input signal (left panels (c) and (e)) and for a speech input (right panels (d) and (f)), respectively. Panel (b) shows the speech input signal that was used to obtain the simulation results in the right panels.

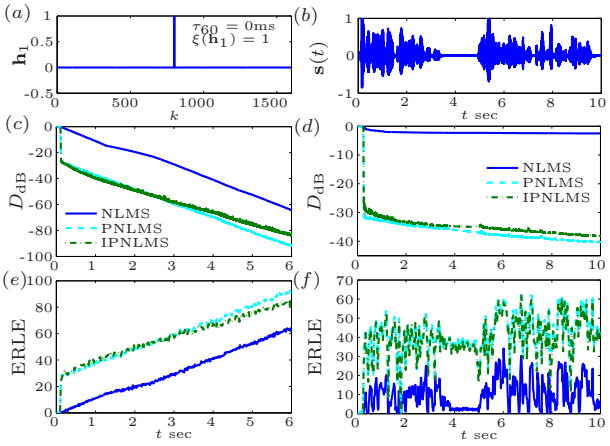

Fig. 6: Comparison of NLMS, PNLMS and IPNLMS algorithms for IR $\mathbf{h}_1$ (delayed delta dunction function also depicted in Fig. 4 (a)).

The performance comparison for the most sparse IR, i.e. the delayed delta function, is shown in Fig. 6. It can be seen that the initial convergence of PNLMS and IPNLMS is much faster than that of the NLMS. Especially for the speech input (right panels) the performance is significantly increased by the proportionate algorithms. Since the PNLMS is optimized for this maximally sparse IR its performance is even better than the performance of the IPNLMS which is more obvious for the speech input signal (right panels) than for the white input signal (left panels).

The simulation results in Figs. 7 and 8 show that the performance of the PNLMS decreases for more

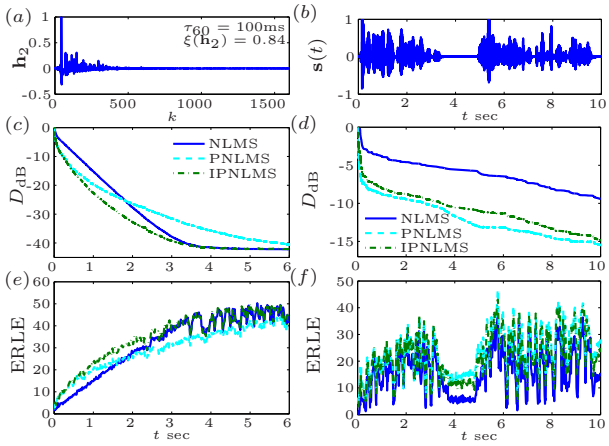

Fig. 7: Comparison of NLMS, PNLMS and IPNLMS algorithms for RIR $\mathbf{h}_2$ ($\tau_{60} = 100$ ms, see also Fig. 4 (b)).

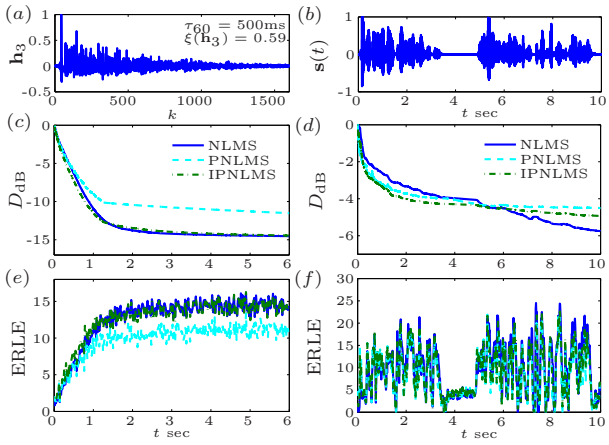

Fig. 8: Comparison of NLMS, PNLMS and IPNLMS algorithms for RIR $\mathbf{h}_3$ ($\tau_{60} = 500$ ms, see also Fig. 4 (c)).

dispersive IRs while the IPNLMS shows a good performance in all scenarios.

Simulation results for the equalized IR of Fig. 4 (d) are shown in Fig. 9. It can be seen that the performance of PNLMS and IPNLMS is similar, but both algorithms outperform the conventional NLMS.

From the previously shown simulation results, it is not difficult to draw the conclusion that PNLMS behaves better than NLMS only if the RIR is sparse, while IPNLMS converges better than PNLMS when

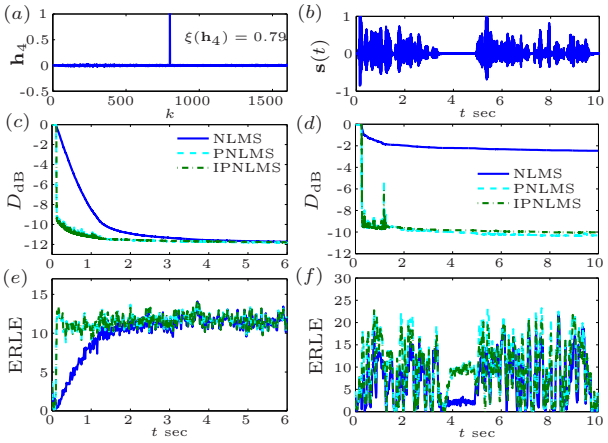

Fig. 9: Comparison of NLMS, PNLMS and IPNLMS algorithms for equalized IR $\mathbf{h}_4$ (see also Fig. 4 (d)).

the RIR is dispersive. Actually, IPNLMS performs best independent of the nature of the RIR for Gaussian white noise excitation. For speech as input signal, IPNLMS with $\alpha = 0$ always leads to a good performance, however, not to the best performance in any case. An optimum α for the IPNLMS depends on the nature of the RIR. However, for equalized IRs such as in Fig. 9 are clearly preferable over conventional update schemes.

5.2. LRC Performance in Dependence of AEC System Distance

Since the LRC filter depends on a reliable estimate $\hat{\mathbf{h}}[k]$ of the RIR to be equalized (cf. Algorithm 1 and Fig. 2) the current convergence state of the *inner AEC* is very important for the LRC filter [9].

The LRC filter's performance is shown in Fig. 10 for different system distances of the *inner AEC* in terms of signal-to-reverberation-ratio enhancement (SRRE)

$$\mathrm{SRRE} = \mathrm{SRR}_{\mathrm{out}} - \mathrm{SRR}_{\mathrm{bypass}} \tag{20}$$

which is defined similarly to the signal to noise ratio enhancement (SNRE) widely used for evaluating noise reduction algorithms [9]. In (20) $\mathrm{SRR}_{\mathrm{out}}$ is the signal-to-reverberation ratio (SRR) after processing by the LRC filter $\mathbf{c}_{\mathrm{EQ}}[k]$ and the RIR $\mathbf{h}[k]$, and $\mathrm{SRR}_{\mathrm{bypass}}$ is the SRR for the case that the LRC filter is set to bypass ($\mathbf{c}_{\mathrm{EQ}}[k] = \mathbf{d}$). $\mathrm{SRR}_{\mathrm{out}}$ and $\mathrm{SRR}_{\mathrm{bypass}}$ are defined as

$$\mathrm{SRR}_{\mathrm{out}} = 10\,\log_{10}\frac{\mathrm{E}\{\hat{y}^2[k]\}}{\mathrm{E}\{(\hat{y}[k]-y[k])^2\}}, \tag{21}$$

$$\mathrm{SRR}_{\mathrm{bypass}} = 10\,\log_{10}\frac{\mathrm{E}\{\hat{y}^2[k]\}}{\mathrm{E}\{(\hat{y}[k]-y_b[k])^2\}}, \tag{22}$$

with $\hat{y}[k]$ being the desired signal at the output of the target system ($\hat{y}[k] = s_f[k] * d[k]$) and $y[k]$ is the microphone signal ($y[k] = s_f[k] * c_{\mathrm{EQ}}[k] * h[k]$). $y_b[k]$ is the output signal when the equalizer switched to bypass ($y_b[k] = s_f[k] * d[k] * h[k]$).

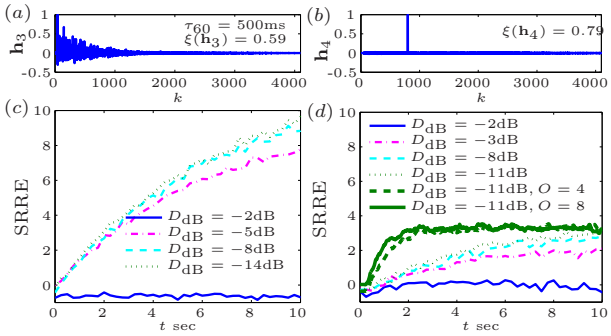

Fig. 10: LRC performance in terms of SRRE obtained by the LRC filter for different system distances D_{dB} of the *inner AEC*. Input signal was white Gaussian noise. Panels (a) and (b) show results for different RIRs.

Fig. 10 shows that the performance of the LRC filter increases with the convergence of the *inner AEC* exemplarily for the two impulse responses of Figs. 4 (c) and (d). If a certain amount of echo cancellation is reached ($D_{\mathrm{dB}} \approx -2$ dB) an enhancement in SSR can be obtained. In panel (d) two additional curves are depicted in thicker lines that show the influence of the overclocking factor O for a relative system distance of $D_{\mathrm{dB}} = -11$ dB. It can be seen that faster convergence of the LRC filter can be obtained by increasing O in Algorithm 1. However, the maximum performance of the LRC filter after convergence is determined by the relative system distance of the *inner AEC* filter D_{dB}.

5.3. Performance of Inner AEC in Dependence of Equalizer

It is known that gradient algorithms for AEC perform better for uncorrelated input signals such as Gaussian white noise. An LRC filter which is located in front of the AEC input signal $x[k]$ will change the signal correlaton, i.e. for a white input signal it will introduce correlation. Fig. 11 shows the performance of the *inner AEC* in terms of relative system distance D_{dB} in panels (c) and (d) for white Gaussian input and for the speech signal, respectively. The corresponding RIR and the speech signal are depicted in panels (a) and (b), respectively.

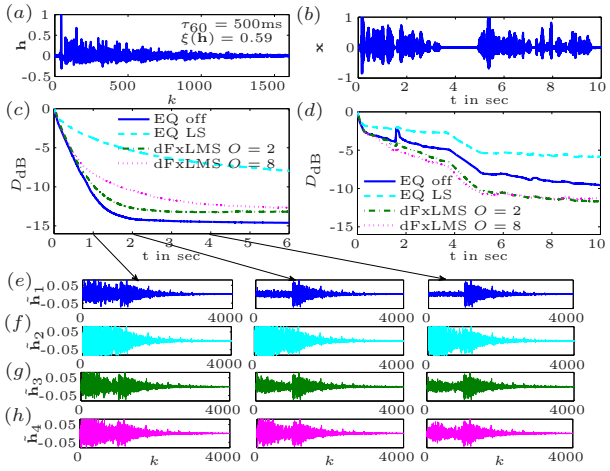

Fig. 11: Performance of *inner AEC* in dependence of different update strategies of the preceeding LRC filter. RIR to be identified is shown in panel (a), system performance in terms of the AEC's relative system distance in panels (c) and (d). Panels (e) to (h) show the respective system misalignment $\tilde{\mathbf{h}}$ at different times and for the different LRC algorithms.

It can be seen that a least-squares equalizer according to (6) leads to a decreased convergence speed compared to an inactive LRC filter for speech as well as for noise. For white noise excitation this is obvious since the filter introduces additional correlation to the AEC input signal $x[k]$. The AEC performance, if the dFxLMS algorithm described in Section 2 is used, is closer to the performance without AEC, for speech input, convergence is even faster than without LRC filter. It seems that the gradient algorithm has a positive effect on the signal's statistical properties here.

For the simulation results for white noise excitation in panel (b) the system distances $\tilde{\mathbf{h}}$ are shown in panels (e), (f), (g) and (h) exemplarily after 1 s, 2 s and 4 s of AEC convergence. If the LRC filter is switched off in (e) it can be clearly observed that the first part up to the coefficient 1023 of the RIR is identified by the AEC filter while the un-modeled tail contributes to the system distance vector $\tilde{\mathbf{h}}$. For the different LRC filter types the AEC system distance vectors $\tilde{\mathbf{h}}$ also have more energy in the early part. Please note, that the system distance vector $\mathbf{h}$ may have significant influence on the target system $\mathbf{g}'[k]$ for the *outer AEC* in (16) if the *outer AEC* uses the error signal $e_{\mathrm{AEC},1}[k]$.

5.4. Performance of Proportionate Update Schemes for Outer AEC

It was shown in Fig. 9 that identification of a perfectly equalized IR can be done efficiently by proportionate update schemes. If the error signal of the *inner AEC* is not used by the *outer AEC*, i.e. switch S_2 in Fig. 5 is in upper position, the system $\mathbf{g}[k]$ to be identified (15) by the *outer AEC* can be assumed to be sparse.

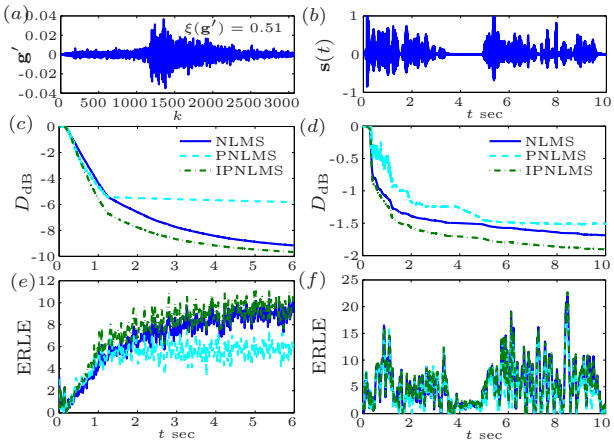

Fig. 12: Comparison of NLMS, PNLMS and IPNLMS for impulse response $\mathbf{g}'[k]$ that may be observed by *outer AEC*.

However, if an *outer AEC* is concatenated to the *inner AEC* to increase the echo reduction, i.e. switch

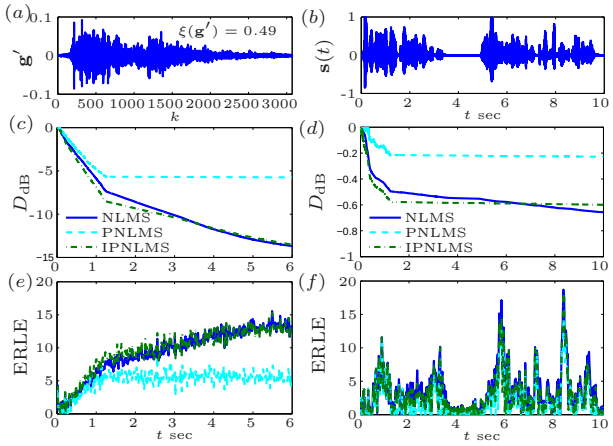

Fig. 13: Comparison of NLMS, PNLMS and IPNLMS for impulse response $\mathbf{g}'[k]$ that may be observed by *outer AEC*.

S_2 in Fig. 5 is in lower position, the *outer AEC* has to identify $\mathbf{g}'[k]$ given in (16). The LRC filter is designed to equalize $\mathbf{h}[k]$, thus the resulting system $\mathbf{g}'[k]$ will not be as sparse as assumed, which could be already observed from the system distance vectors in panels (e)-(h) of Fig. 11. Figs. 12 and 13, thus, show the performance of NLMS, PNLMS and IPNLMS for two systems $\mathbf{g}'[k]$ exemplarily, one obtained using white noise input after sufficient convergence of the *inner AEC* (Fig. 12) and one for speech input after partly convergence of the *inner AEC* (Fig. 13). Although the system to be identified is not really sparse especially in Fig. 13 the IPNLMS is still a good choice.

For evaluation if an *outer AEC* should rely on the error signal of the *inner AEC* or work independently these two systems are compared in Fig. 14. If the *outer AEC* directly depends on the error signal of the *inner AEC* the total ERLE of the combined system $\mathrm{ERLE}_{\mathrm{total}}$ can be calculated from the ERLE_1 achieved by the *inner AEC* and ERLE_2 achieved by the *outer AEC* as depicted in Fig. 14.

$$\mathrm{ERLE}_1 = 10\,\log_{10}\frac{\mathrm{E}\{\psi^2[k]\}}{\mathrm{E}\{e^2_{\mathrm{AEC},1}[k]\}} \tag{23}$$

$$\mathrm{ERLE}_2 = 10\,\log_{10}\frac{\mathrm{E}\{e^2_{\mathrm{AEC},1}[k]\}}{\mathrm{E}\{e^2_{\mathrm{AEC},2}[k]\}} \tag{24}$$

$$\begin{aligned}\mathrm{ERLE}_{\mathrm{total}} &= \mathrm{ERLE}_1 + \mathrm{ERLE}_2 \\ &= 10\,\log_{10}\frac{\mathrm{E}\{\psi^2[k]\}}{\mathrm{E}\{e^2_{\mathrm{AEC},2}[k]\}}\end{aligned} \tag{25}$$

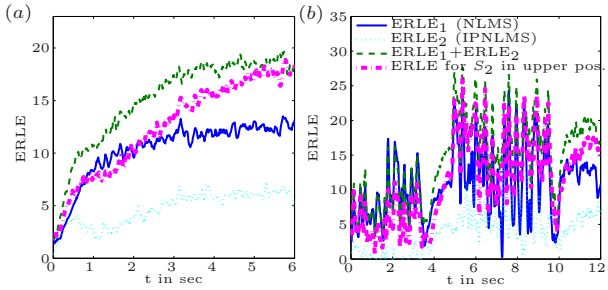

Fig. 14: AEC performance comparison for system consisting of outer AEC and inner AEC for the two possible combination shown in Fig. 5 (AEC filter lengths were $L_{\mathrm{AEC},1} = 1024$ and $L_{\mathrm{AEC},2} = 2048$).

It can be seen from Fig. 14 that although the IR to be identified by the *outer AEC* $\mathbf{g}'[k]$ may not always be sparse the system that exploits echo reduction of both filters (switch S_2 in Fig. 5 is in lower position) leads to a higher amount of echo reduction. At all the AEC performance has been increased by about 50% by adding an *outer AEC*.

The previous simulation results showed that a combined system of *inner AEC* and *outer AEC* relying on the error signal $e_{\mathrm{AEC},1}[k]$ which is upated by the IPNLMS algorithm shows good performance for sparse IRs and even if the system $\mathbf{g}'[k]$ is not always sparse, e.g. in periods of convergence of *inner AEC* or LRC filter. One further advantage of the proportionate update schemes is, that their convergence speed can be increased by a higher stepsize $\mu[k]$. This will be visualized in Fig. 15 for a white Gaussian excitation $s_f[k]$ and in Fig. 16 for speech as input $s_f[k]$. The convergence of the *inner AEC* is depicted in terms of relative system distance $D_{1,\mathrm{dB}}$ in panels (b) of Fig. 15 and 16. The corresponding system distance vector $\tilde{\mathbf{h}}_1$ is depicted exemplarily for time instances $\{1, 3, 5, 8, 10\}$ s in panels (c). Since the *outer AEC* has to identify the system $\mathbf{g}'[k] = \mathbf{C}_{\mathrm{EQ}}[k]\left(\mathbf{h}[k] - \left[\mathbf{c}^T_{\mathrm{AEC},1}[k], \mathbf{0}^T\right]^T\right)$ the equalizer coefficients are shown in panels (d) and the system $\mathbf{g}'$ in panels (e) at the respective time instances.

Panels (f) show the performance of the LRC filter in terms of SRR_{out} and SRRE and panels (g) compare NLMS, PNLMS and IPNLMS for the *outer AEC* in the proposed system when all three adaptive filters are active.

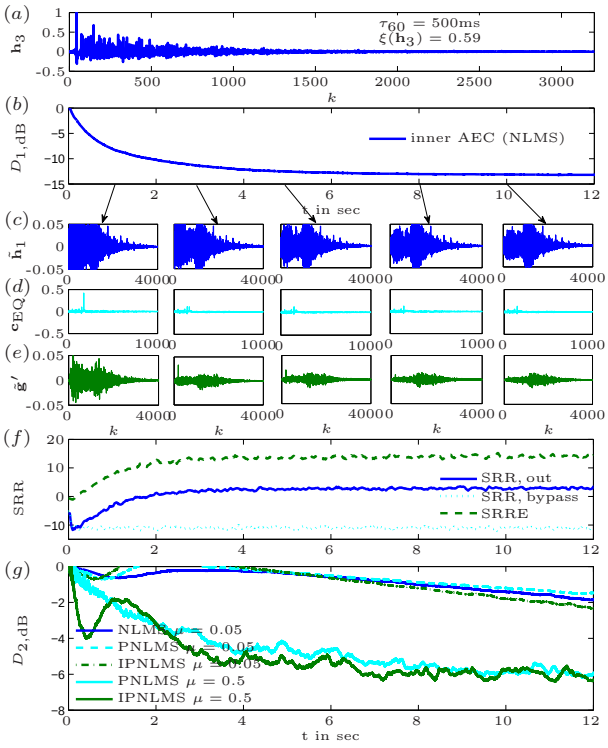

Fig. 15: Performance of combined system as shown in Fig. 5 (switch S_2 in lower position) for white noise as input. (a) the RIR; (b) relative system distance $D_{1,\text{dB}}$ of inner AEC; (c) system distance vector $\tilde{\mathbf{h}} = \mathbf{h}[k] - \mathbf{c}_{\text{AEC}_1}[k]$ of AEC_1 after $\{1, 3, 5, 8, 10\}$ seconds; (d) corresponding equalizer coefficients $\mathbf{c}_{\text{EQ}}[k]$; (e) IR to be identified by *outer AEC* $\mathbf{g}'[k]$ for AEC_2; (f) SSRR and SSRE achieved by LRC filter; (g) system distance of *outer AEC*.

If the step-size $\mu[k]$ is considered to be the same for NLMS, PNLMS and IPNLMS $\mu = 0.05$ was fund to be the highest possible step-size for the *outer AEC* to work for all algorithms. Here the NLMS is the limiting algorithm while for PNLMS and IPNLMS higher step-sizes can be chosen. As it can be seen from Figs. 15 and 16 the use of PNLMS and IPNLMS already achieves slight performance gains if the same step-size is chosen. If the step-size is increased for

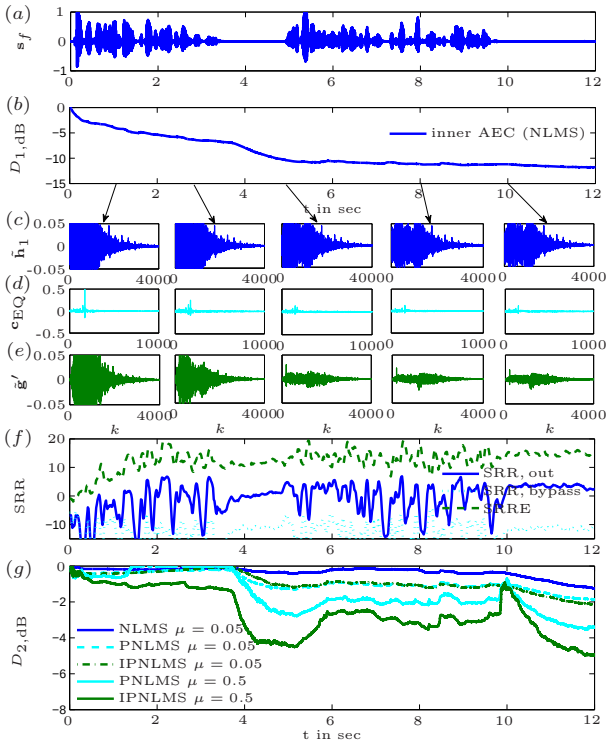

Fig. 16: Performance of combined system as shown in Fig. 5 (switch S_2 in lower position) for speech as input. (a) speech input signal; (b) relative system distance $D_{1,\text{dB}}$ of inner AEC; (c) system distance vector $\tilde{\mathbf{h}} = \mathbf{h}[k] - \mathbf{c}_{\text{AEC}_1}[k]$ of AEC_1 after $\{1, 3, 5, 8, 10\}$ seconds; (d) corresponding equalizer coefficients $\mathbf{c}_{\text{EQ}}[k]$; (e) IR to be identified by *outer AEC* $\mathbf{g}'[k]$ for AEC_2; (f) SSRR and SSRE achieved by LRC filter; (g) system distance of *outer AEC*.

PNLMS and IPNLMS (which is not possible for NLMS) the performance can be further increased.

6. CONCLUSION

In this contribution, a combined system for hands-free communication has been proposed and evaluated using a listening-room-compensation filter for reverberation reduction and a two stage acoustic echo cancellation system. Proportionate LMS filter update schemes were evaluated for the identification of equalized acoustic channels. Simulation results showed that the proposed system of LRC filter and

two-stage AEC performed best if proportionate update strategies like the PNLMS or IPNLMS were used. Here, the IPNLMS was more robust in terms of performance for arbitrary impulse responses and, thus, should be the algorithm of choice for identification of equalized impulse responses.

7. ACKNOWLEDGEMENT

Work was supported in parts by German Research Foundation DFG under Grants Ka841-17 and Me1170/3.

8. REFERENCES

[1] E. Hänsler and G. Schmidt (Eds.), *Speech and Audio Processing in Adverse Environments*, Springer, 2008.

[2] A. Mader, H. Puder, and G. Schmidt, "Step-Size Control for Acousatic Echo Cancellation Filters – an Overview," *Elsevier Signal Processing*, vol. 80, no. 9, pp. 1697–1719, September 2000.

[3] J. B. Allen, "Effects of Small Room Reverberation on Subjective Preference," *Journal of the Acoustical Society of America (JASA)*, vol. 71, no. S1, p. S5, 1982.

[4] P.A. Naylor and N.D. Gaubitch, "Speech Dereverberation," in *Proc. Int. Workshop on Acoustic Echo and Noise Control (IWAENC)*, Eindhoven, The Netherlands, Sept. 2005.

[5] S. J. Elliott and P. A. Nelson, "Multiple-Point Equalization in a Room Using Adaptive Digital Filters," *Journal of the Audio Engineering Society*, vol. 37, no. 11, pp. 899–907, Nov. 1989.

[6] J. N. Mourjopoulos, "Digital Equalization of Room Acoustics," *Journal of the Audio Engineering Society*, vol. 42, no. 11, pp. 884–900, Nov. 1994.

[7] S. Goetze, M. Kallinger, A. Mertins, and K.-D. Kammeyer, "Multi-Channel Listening-Room Compensation using a Decoupled Filtered-X LMS Algorithm," in *Proc. Asilomar Conf. on Signals, Systems, and Computers*, Pacific Grove, USA, pp. 811–815, Oct. 2008.

[8] T. Hikichi, M. Delcroix, and M. Miyoshi, "Inverse Filtering for Speech Dereverberation Less Sensitive to Noise and Room Transfer Function Fluctuations," *EURASIP J. on Advances in Signal Processing*, vol. Volume 2007, Article ID 34013, 2007, doi:10.1155/2007/34013.

[9] S. Goetze, M. Kallinger, A. Mertins, and K.-D. Kammeyer, "System Identification for Multi-Channel Listening-Room Compensation using an Acoustic Echo Canceller," in *Workshop on Hands-free Speech Communication and Microphone Arrays (HSCMA)*, Trento, Italy, pp. 224–227, May 2008.

[10] D.L. Duttweiler, "Proportionate Normalized Least-Mean-Squares Adaptation in Echo Cancelers," *IEEE Trans. on Speech and Audio Processing*, vol. 8, no. 5, pp. 508–517, 2000.

[11] S.L. Gay, "An Efficient, Fast Converging Adaptive Filter for Network Echo Cancellation," in *Proc. Asilomar Conf. on Signals, Systems, and Computers*, Pacific Grove, CA, USA, pp. 394–398, Nov. 1998.

[12] J. Benesty and S.L. Gay, "An Improved PNLMS Algorithm," in *Proc. IEEE Int. Conf. on Acoustics, Speech, and Signal Processing (ICASSP)*, Orlando, FL, USA, pp. 1881–1884, May 2002.

[13] J. Benesty, Y. Huang, J. Chen, and P.A. Naylor, "Adaptive Algorithms for the Identification of Sparse Impulse Responses," in *Topics in Acoustic Echo and Noise Control*, E. Hänsler and G. Schmidt, Eds., chapter 5, pp. 125–153. Springer, Berlin, 2006.

[14] J. Benesty, T. Gänsler, D. R. Morgan, M. M. Sondhi, and S. L. Gay, *Advances in Network and Acoustic Echo Cancellation*, Springer, Berin, 2001.

[15] S. T. Neely and J. B. Allen, "Invertibility of a Room Impulse Response," *Journal of the Acoustical Society of America (JASA)*, vol. 66, pp. 165–169, July 1979.

[16] A.W.H. Khong, X. Lin, and P.A. Naylor, "Algorithms for Identifying Clusters of Near-Common Zeros in Multichannel Blind System

Identification and Equalization," in *Proc. IEEE Int. Conf. on Acoustics, Speech, and Signal Processing (ICASSP)*, Las Vegas, NV, USA, pp. 389–392, Mrz 2008.

[17] B. D. Radlović, R. C. Williamson, and R. A. Kennedy, "Equalization in an Acoustic Reverberant Environment: Robustness Results," *IEEE Trans. on Speech and Audio Processing*, vol. 8, no. 3, pp. 311–319, May 2000.

[18] S. Goetze, E. Albertin, M. Kallinger, A. Mertins, and K.-D. Kammeyer, "Quality Assessment for Listening- Room Compensation Algorithms," in *Proc. IEEE Int. Conf. on Acoustics, Speech, and Signal Processing (ICASSP)*, Dallas, Texas, USA, March 2010.

[19] S. Goetze, E. Albertin, J. Rennies, E.A.P. Habets, and K.-D. Kammeyer, "Speech Quality Assessment for Listening-Room Compensation," in *38th AES Conference*, Pitea, Sweden, July 2010.

[20] B. Widrow and S.D̃. Stearns, *Adaptive Signal Processing*, Englewood Cliffs, 1985.

[21] S. Goetze, M. Kallinger, A. Mertins, and K.-D. Kammeyer, "A Decoupled Filtered-X LMS Algorithm for Listening-Room Compensation," in *Proc. Int. Workshop on Acoustic Echo and Noise Control (IWAENC)*, Seattle, USA, Sept. 2008.

[22] Alfred Mertins, Tiemin Mei, and Markus Kallinger, "Room Impulse Response Shortening/Reshaping with Infinity- and p-Norm Optimization," *IEEE Trans. on Audio, Speech and Language Processing*, vol. 18, no. 2, pp. 249–259, Feb. 2010, DOI:10.1109/TASL.2009.2025789.

[23] E. Bjarnason, "Active Noise Cancellation using a Modified Form of the Filtered-X LMS Algorithm," in *Proc. EURASIP European Signal Processing Conference (EUSIPCO)*, Brussels, Belgium, 1992, pp. 1053–1056.

[24] S. Goetze, M. Kallinger, A. Mertins, and K.-D. Kammeyer, "Estimation of the Optimum System Delay for Speech Dereverberation by Inverse Filtering," in *Int. Conf. on Acoustics (NAG/DAGA 2009)*, Rotterdam, The Netherlands, Mrz 2009, pp. 976–979.

[25] S. Haykin, *Adaptive Filter Theory*, Prentice Hall, 2002.

[26] C. Breining, P. Dreiseitel, E. Hänsler, A. Mader, B. Nitsch, H. Puder, T. Schertler, G. Schmidt, and J. Tilp, "Acoustic Echo Control – An Application of Very-High-Order Adaptive Filters," *IEEE Signal Processing Magazine*, pp. 42–69, July 1999.

[27] S. Goetze, M. Kallinger, A. Mertins, and K.-D. Kammeyer, "Least Squares Equalizer Design under Consideration of Tail Effects," in *Proc. German Annual Conference on Acoustics (DAGA)*, Stuttgart, Germany, pp. 599–600, March 2007.

[28] P.A. Naylor, J. Cui, and M. Brookes, "Adaptive Algorithms for Sparse Echo Cancellation," *ITSP*, vol. 86, no. 6, pp. 1182–1192, 2006.

[29] Y. Kaneda, S. Makino, and N. Koizumi, "Exponentially Weighted Step–Size NLMS Aaptive Filter Based on the Statistics of a Room Impulse Response," *IEEE Trans. on Speech and Audio Processing*, vol. 1, no. 1, pp. 101–108, Jan 1993.

[30] H. Deng and M. Doroslovački, "Improving Convergence of the PNLMS Algorithm for Sparse Impulse Response Identification," *IEEE Signal Processing Letters*, vol. 12, no. 3, pp. 181–184, Mrz 2005.

[31] Jacob Benesty and Thomas Gänsler, "A Multi-Channel Acoustic Echo Canceler Double-Talk Detector Based on a Normalized Cross-Correlation Matrix," *Eur. Trans. Telecomm.*, vol. 13, March 2002.